LASER WAKEFIELD ACCELERATION USING A LASER PRODUCED ALUMINIUM PLASMA*

Jaehoon Kim#, Younghoon Hwangbo, Seok-Gy Jeon, KERI, Ansan, Korea
Woo Je Ryu, Kyung Nam Kim, Seong Hee Park, Nikolay Vinokurov, KAERI, Daejeon, Korea

Abstract

In laser wakefield accelerator, usually a gas target is used to generate plasma medium. With this gas target, the pressure of the system cannot be keep as low as possible for electron beam application such as seeding the storage ring. To reduce this vacuum problem in LWFA, a plasma generated from solid Al target was used as plasma medium. A fundamental beam from the Q-switched ns pump laser in the Ti:sapphire power amplifier was used to generate a plasma from solid Al target. The plasma density was controlled by changing the distance between the main laser pulse for electron acceleration and the solid target. The plasma density was measured by the interferometer. The measured density indicates that the average charge of the ion in pre-plasma was 4.4. The main pulse ionized the Al plasma up to Al XII which means that the ionization injection could be used as an injection scheme. A 28 TW fs laser was used to accelerate the electron. A quasi-monochromatic electron was generated. The peak energy was 70 MeV and energy spread was 15 %. The divergence of the beam was 12 mrad in horizontal direction and 6 mrad in vertical direction.

INTRODUCTION

An interaction between ultrahigh intensity fs laser and plasma can be used as an electron accelerator which is called as a laser wakefield accelerator (LWFA) [1]. Due to the development of the chirped pulse amplification (CPA) technology, a compact table top ultrahigh intensity fs laser is available [2,3]. The feasibility of LWFA to accelerate the electron is already demonstrated. The main difference between the LWFA and conventional electron accelerator is the acceleration media. In LWFA, a plasma is used as acceleration medium, and such medium can support much higher acceleration field. A compact high energy electron accelerator is possible due to this strong acceleration field in LWFA. Besides the small system size, LWFA can generate a very short femtosecond time scale electron bunches because the acceleration region is very narrow [4]. The measured electron bunch length was less than 50 fs which was measured by using the coherent radiation transition[5,6]. A femtosecond x-ray can be generated using these femtosecond electron bunches which is very useful for the measurement of the dynamics of materials in femtosecond time scale [7-9].

In LWFA, typically a gas target is used to generate a plasma medium for the acceleration. But in vacuum sensitive applications such as an injector for a storage ring, the gas nozzle is not feasible because the gas injected into the vacuum chamber increases the pressure of the whole system. A plasma generated from a solid target can be used such an application because the number of particle injected into the vacuum chamber is much less than gas target. With solid target, the method to control the plasma density is needed because the plasma generated from a solid target by a laser expands very fast [10].

In this work, the feasibility of the laser produced plasma from solid target as an acceleration medium for a laser wakefield acceleration was studied. A density of the plasma was controlled by the distance between the main laser and the target and it was measured by using a Nomarski interferometer. The experimental results show that a laser produced plasma can be a good candidate of the acceleration medium for LWFA in vacuum sensitive applications.

EXPERIMENT

To remove vacuum problem in LWFA with gas target, a plasma generated from a solid target was used as an acceleration medium for the LWFA. The experimental setup is shown in Fig. 1. The residual fundamental laser beam after the second harmonic generation from the pump laser of the main amplifier in the Ti:sapphire laser was used to generate a pre-plasma. By this method, the other laser is not needed to generate the pre-plasma. The laser was focused in line at a pure Al target by using a cylindrical lens and a biprism. The biprism was used to generate a uniform line intensity. If the intensity of the pre-pulse is too high, the plasma density at the interaction is too low because of the fast plasma expansion [10]. The size of the solid target is 2 mm wide and 25 mm long. After each laser shot, the target was moved 1 mm in x direction to supply a fresh surface. The laser line width at the target was controlled by the distance between the target and the cylindrical lens. In this experiments, the line width was 0.7 mm.

A ultrahigh intensity Ti:sapphire laser was used to accelerate electrons. The pulse duration of the laser was 25 fs and the peak power was 28 TW. The laser was focused at the pre-plasma by an off-axis parabolic mirror. The focal length of the OAP was 326 mm. The measured laser spot size was 5.4 µm. The time delay between the pre- and main pulse was fixed due to the optical pass length and was 140 ns.

The density of the pre- and main plasma was measured by using a Nomarski interferometer. A parts of the main pulse is used as a probe pulse after converted to the second harmonic pulse. A fast Fourier transform was used

---

#jkim@keri.re.kr

ISBN 978-3-95450-134-2

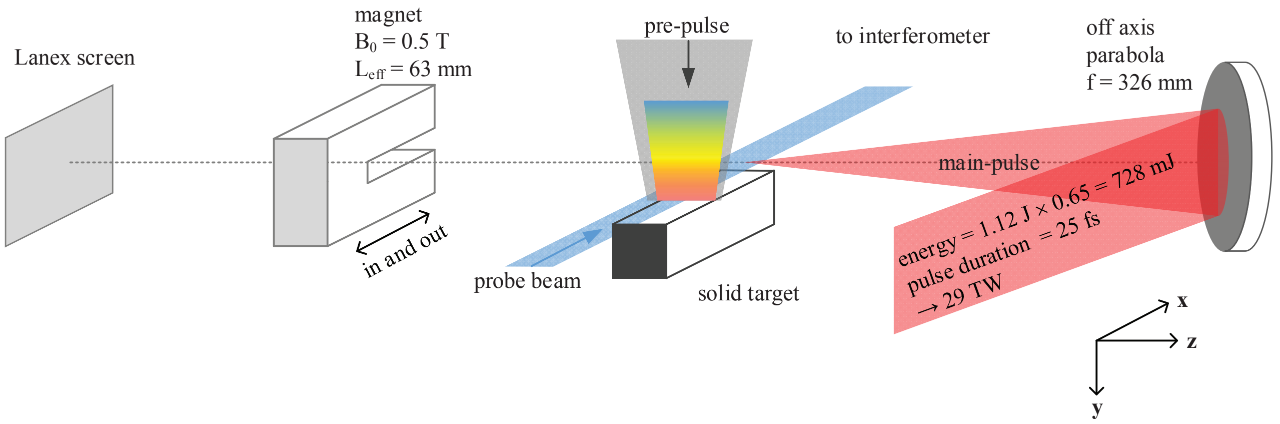

Figure 1: Experimental setup. A ns pre-pulse is from the fundamental laser of the pump laser for the amplifier of Ti:sapphire laser system. A pure Al target is on the 3-axis stage to control the position of the target relative to the laser beam. Some parts of the fs laser beam is used as a probe beam for the interferometer shown as blue line. Bending magnet is used to measure the electron beam energy. The peak power of the main pulse is 29 TW.

to recover the phase change due to the plasma [11]. The density was measured by using an Abel inversion [12].

After the target, an integrated current transformer was used to measure the bunch charge and after that a Lanex film was placed to measure the shape of the electron beam. A dipole mount was used to measure the energy of the beam by bending the electron. The magnetic field strength at the center of the pole was 0.5 T. The CCD camera was used to record the image of the Lanex.

RESULTS

Profiles of the pre- and main plasma were measured by interferometer. The density profiles are shown in Fig. 2. Uniform pre-plasma was generated due to the focusing optics for the ns laser as shown in Fig. 2-a). Due to the target width, the length of the pre-plasma is 2 mm. The density profile at 0.5 mm from the target surface is shown as a blue dashed line in Fig. 2-c). When the main pulse focused at the pre-pulse, the density profile was changed as in Fig. 2-b). The distance between the target and the main pulse was 0.5 mm. The profile of the main plasma density at 0.5 m from the target is shown in Fig. 2-c) with red solid line. The density of the main plasma increased because the main pulse ionized the ion in the pre-plasma. The density at the center of the plasma were 4×10^{18} cm^{-3} for pre-plasma and 1.6×10^{19} cm^{-3} for main plasma. Comparing the density profile of the pre- and main plasmas, the average charge of the ion in pre-plasma was 4.4 which means that the initial ionization of the plasma Al V.

The main pulse ionized the Al plasma up to Al XII by the optical field ionization. The density was very sensitive to the distance between the main laser and the target because the density exponentially decreased along the normal direction to the target.

Figure 3 show the electron beam profile and the energy distribution. The generation of the beam was very sensitive to the distance between the target and the main pulse. The electron beam was generate only when this distance was 0.5 mm due to the fast expansion of the plasma generated from the solid target. If the distance is longer than 0.5 mm, the density is too low. If that is shorter than 0.5 mm, the density is too high. The electron beam shape is elongated in horizontal direction.

As shown in Fig. 3-a), the beam divergence is 12 mrad in horizontal direction and 6 mrad in vertical direction. Blue dots in Fig. 3-a) show the center of the beam for each measurement. From this measurement, the pointing stability of the beam is 2 mrad in horizontal and 3.3 mrad in vertical direction.

Figure 3-b) shows the measured electron energy distribution. Quasi mono-energetic electron beams are generated by this solid target scheme. The average peak energy over 5 shots is 46 ± 3 MeV. The bunch charge is 13 ± 2 pC. The best electron beam generated from this scheme is the beam with peak energy 70 MeV and 15 % energy spread. With this result, the solid target can be used to accelerate electrons in LWFA.

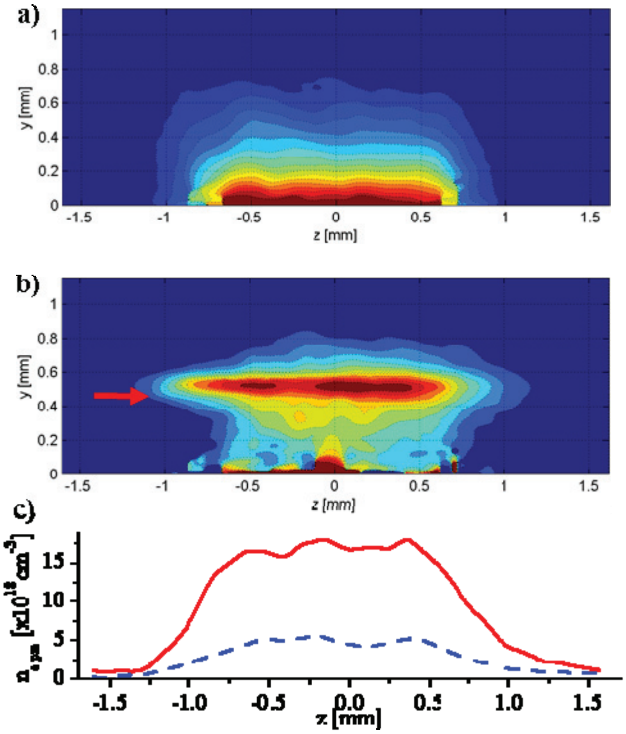

Figure 2: Plasma density profile. Density profile of the pre-plasma is shown in a) and the main plasma shown in b). A red arrow at b) indicates the positon of the main pulse. The cross sectional view of the density profile in shown in c).

CONCLUSION

To reduce the effect of the gas to the vacuum chamber for the vacuum sensitive application in LWFA, a plasma generated from solid Al target was used as plasma medium. A ns YAG laser was used to generate pre-plasma from the Al target. Due to the rapid expansion of the plasma, the plasma density was controlled by changing the distance between the main laser pulse for electron acceleration and the solid target. The electron beam was generate when the distance between the main and the target was 0.5 mm. The generation of the beam was sensitive to this distance because the plasma density. The plasma density was measured by the interferometer. A 29 TW fs laser was used to accelerate the electron. A quasi-monochromatic electron was generated. The peak energy was 70 MeV and energy spread was 15 %. The divergence of the beam was 12 mrad in horizontal direction and 6 mrad in vertical direction. The electron beam generated with this scheme will be used as the injector for the storage ring to generate strong THz radiation.

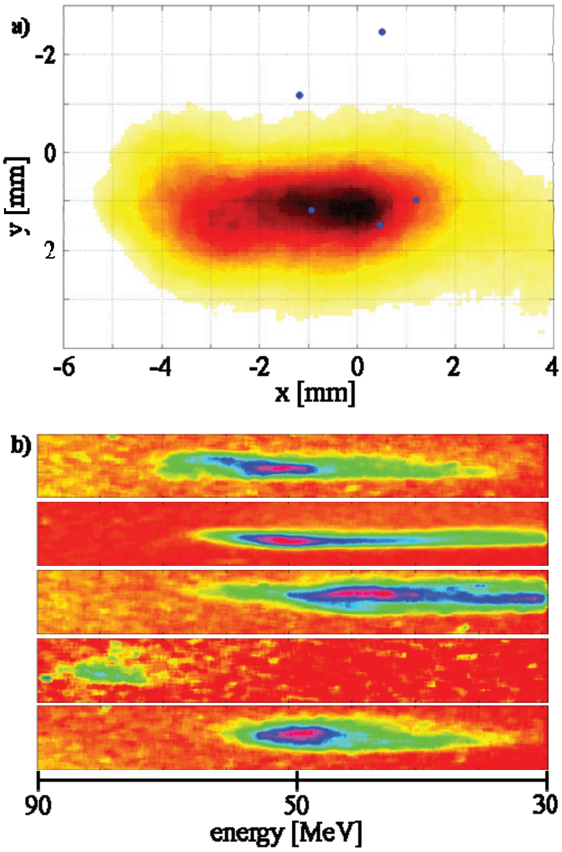

Figure 3: Accelerated beam image and the energy distribution. The beam shape and the center of the beams are shown in a). The measured electron energy in 5 series experiments are shown in b).

REFERENCES

[1] T. Tajima, and J. M. Dawson, Phys. Rev. Lett. 43, 267 (1979).

[2] D. Strickland and G. Mourou, Opt. Commun. 56, 219 (1985).

[3] P. Maine, D. Strickland, P. Bado, M. Pessot, and G. Morou, IEEE J. Quantum Electron. 24, 398 (1988).

[4] E. Esarey, P. Sprangle, J. K. Krall, and A. Ting, IEEE Trans. Plas. Sci. 24, 252 (1996).

[5] W. P. Leemans, J. van Tilborg, J. Faure, c. G. R. Geddes, C. Toth, C. B. Schroeder, E. Esarey, and G. Fubiani, Phys. Plasma 11, 2899 (2004).

[6] J. van Tilborg, C. B. Schroeder, C. V. Filip, C. Toth, C. G. R. Geddes, G. Fubiani, R. Huber, R. A. Kaindl, E. Esarey, and W. P. Leemans, Phys. Rev. Lett. 96, 014801 (2006).

[7] C. Rose-Petrucks, R. Jimenez, T. Guo, A. Cavalleri, C. W. Siders, F. Raksi, J. A. Squier, B. C. Walker, K. R. Wilson, and C. P. J. Barty, Nature 398, 310 (1999).

[8] C. Rischel, A. Rousse, I. Uschmann, P.-A. Albouy, J.-P. Geindre, P. Audebert, J.-C. Gauthier, E. Forster, J.-L. Martin, and A. Antonetti, Nature 390, 490 (1997).

[9] J. Kim, H. Jang, S. Yoo, M. Hur, I. Hwang, J. Lim, V. Kulagin, H. Suk, I. W. Choi, N. Hafz, H. T. Kim, K.-H. Hong, T. J. Yu, J. H. Sung, T. M. Jeong, Y.-C. Noh, D.-K. Ko and J. Lee, J. Korean Phys.Soc. 51,397 (2007).

[10] D. Giuliettie and L. A., Gizzi, La Rivista del Nuovo Cimento **21**, 1 (1998).
[11] K. A. Nugent, Appl. Opt. 18, 3101 (1985).
[12] M. Kalal and K. A. Nugent, Appl. Opts. 27, 1956 (1988).

ISBN 978-3-95450-134-2